STABILIZATION OF RUTILE TiO$_2$ NANOPARTICLES WITH GLYMO IN POLYACRYLIC CLEAR COATING

STABILIZACIJA RUTIL TiO$_2$ NANODELCEV Z GLYMO V POLIAKRILNEM TRANSPARENTNEM PREMAZU

Jerneja Godnjavec[1], Bogdan Znoj[1,2], Jelica Vince[2], Miha Steinbucher[2], Andrej Žnidaršič[3], Peter Venturini[1,2]

[1]Center of Excellence for Polymer Materials and Technologies, Tehnološki park 24, 1000 Ljubljana, Slovenia
[2]Helios Group, Količevo 2, 1230 Domžale, Slovenia
[3]Kolektor Nanotesla Institut Ljubljana, Stegne 29, 1521 Ljubljana, Slovenia
jerneja.godnjavec@polimat.si

Titanium dioxide (TiO$_2$), in the crystal form of rutile with high refractive index, 2.7, is one of the most important inorganic pigments. In the recent years nano TiO$_2$ has attracted interest as an inorganic material for nanocomposites. It is used for the development of photocatalysts[1,2], semiconductors in solar cells[3,4] and for the protection of materials from UV damage[5–8].
To achieve high UV absorbing efficiency of TiO$_2$ nanoparticles into polymer matrix and to yield a better compatibility with polymeric materials surface treatment of TiO$_2$ nanoparticles with 3-glycidyloxypropyltrimethoxysilane (GLYMO) in a polyacrylic clear coating was investigated. The grafting of GLYMO on the TiO$_2$ nanoparticles surface was characterized with TGA and FTIR techniques. The stability of TiO$_2$ nanoparticles in a acrylic clear coating was evaluated by zeta potential measurement. Microstructural analysis of nanoparticles was done by SEM and the influence of surface treatment on stability of nanoparticles in dispersion and acrylic coating was analysed. Finally the UV absorption effectivness of acrylic clear coating with treated nanoparticles of rutile TiO$_2$ was measured to determine the effect of improved dispersion. The performance of nanocomposite coatings was demonstrated trough accelerated weathering by gloss measurement. The results showed that surface treatment of TiO$_2$ nanoparticles with GLYMO improves nanoparticles dispersion and preserves UV protection of the acrylic clear coating.

Keywords: titanium dioxide, nanoparticles, polyacrylic clear coating, surface treatment, GLYMO, UV protection

Titanov dioksid (TiO$_2$), v rutilni kristalni obliki z visokim lomnim količnikom, 2.7, je eden najbolj pomembnih anorganskih pigmentov. V zadnjih letih je nano TiO$_2$ pritegnil pozornost kot anorganski material za nanokompozite. Uporablja se za razvoj fotokatalizatorjev[1,2], polprevodnikov in soalrnih celic[3,4] in za UV zaščito materialov[5–8].
Da bi dosegli ustrezno dispergiranje TiO$_2$ nanodelcev v polimerni matrici in boljšo kompatibilnost s polimernimi materiali smo preiskovali površinsko obdelavo TiO$_2$ nanodelcev v poliakrilnem transparentnem premazu. Za optimizacijo dispergiranja je bila površina nanodelcev obdelana z 3-glicidiloksipropiltrimetoksisilanom (GLYMO). Pripenjanje GLYMO na površino TiO$_2$ nanodelcev smo ovrednotili z termogravimetrično analizo (TGA) in s FTIR spektroskopsko analizo. Stabilnosti TiO$_2$ nanodelcev v akrilnem transparentnem premazu smo analizirali z meritvijo zeta potenciala. Mikrostrukturno analizo nanodelcev izvedli s SEM. Na koncu smo analizirali učinkovitost UV absorpcije akrilnega transparentnega premaza z površinsko obdelanimi rutil TiO$_2$ nanodelci, da bi določili efekt izboljšane disperzibilnosti. Z izpostavo pospešenega staranja smo določili funkcionalnost nanokompozitnih premazov na osnovi meritve sijaja. Rezultati so pokazali da površinska obdelava TiO$_2$ nanodelcev z GLYMO izboljša disperziblnost nanodelcev in ohrani UV zaščito akrilnega transparentnega premaza.

Ključne besede: titanov dioksid, nanodelci, poliakrilni transparentni premaz, površinska obdelava, GLYMO, UV zaščita

1 INTRODUCTION

Architectural coatings are usually used to enhance the durability of wood in exterior environment. Inorganic UV absorbers are often used in coatings formulations, since they increase polymer stability. TiO$_2$ possesses a lot of attracting advantages, like thermal stability and long-term life time, compared to traditional organic UV absorbers[9,10].

There are two limitations of using TiO$_2$ as UV absorber. First, TiO$_2$ particularly in anatase crystale form and less in rutile form exhibits strong photocatalytic behavior when absorbing UV-rays, which is harmful for the photostability of polymer materials[5]. As a result, TiO$_2$ nanoparticles as catalyst can create , which can produce highly reactive free radicals and exert strong oxidizing power.

Second, for producing suitable nanocomposites, it is necessary to disperse the nano-particles without agglomeration in organic binders[11,12]. Due to their extremly large surface-area/particle-size ratio, nano-particles have high tendency of agglomeration[13]. Many efforts have been taken in order to overcome the problem of agglomeration. Polymeric dispersants containing different functional groups are usuallly used in order to prevent the high tendency of nanoparticles to form aggregates in the wet state of coating and in the dry paint film. Polyacrylic acid, polyacrylamide and their copolymers are widely used to disperse inorganic particles in aqueous film[14]. Recently, to suppress the photocatalytic property of TiO$_2$, usually silica[15–17] or silane[18–20] were coated onto TiO$_2$ cores. Kang et al. suppressed the photocatalytic property of a TiO$_2$ by coating them with the SiO$_2$ shell in chloroform[17]. Toni et. al. coated dense

SiO$_2$ shells onto TiO$_2$ particles by seeded sol–gel process of tetraethyl silicate (TEOS) in ethanol[16]. The use of different coupling agents such as trialkoxy silanes for surface modification of nanoparticles is recommended. For example, Ukaji et. al. coated thin aminoethylamino-propyltrimethoxysilane layers onto TiO$_2$ particles in ethanol by adding silane during ball-milling dispersing procedure[8]. Shafi et. al. coated octadecyltrihydrosilane layers on TiO$_2$ surfaces in heptane by ultrasonic irradi-ation[21]. M. Sabzi et. al. showed that surface treatment of TiO$_2$ with aminopropyl trimethoxysilane improves nano-particles dispersion and UV protection of the urethane clear coating[22].

The purpose of this study was to investigate the influence of TiO$_2$ nanoparticles surface modifiction by different wt. % of 3-glycidyloxypropyltrimethoxysilane on transparency and UV absorbing efficiency of poly-acrylic coating.

2 EXPERIMENTAL WORK

2.1 Synthesis of TiO₂ nano crystalline particles in rutile crystal structure and preparation of a disper-sion

TiO$_2$ nanoparticles with rutile crystal structure were prepared by co-precipitation method which is described elsewhere[23]. Deagglomerated rutile nanoparticles were prepared as dispersion in water and propilenglycol in high-energy horizontal attrition mill.

2.2 Surface modification of TiO₂ nanoparticles in dispersion with silane coupling agent

As silane coupling agent we used 3-glycidyloxy-propyltrimethoxysilane (GLYMO) with chemical for-mula

$$CH_2-CH-CH_2O-(CH_2)_3Si(OCH_3)_3$$
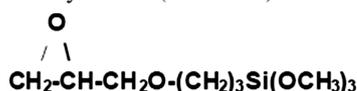
which is a bifunctional organosilane, possessing reactive organic epoxide and hydrolyzable inorganic metoxysilyl groups. It bounds chemically to both inorganic material and organic polymers. According to the producer in the presence of water the methoxy groups hydrolyze to form reactive silanol groups which bound to inorganic substance[24].

We prepared dispersions of TiO$_2$ nanoparticles grafted with GLYMO according to the following

Table 1: Weight ratio of GLYMO and nano TiO₂, dispersed in water
Tabela 1: Utežno razmerje GLYMO in nano TiO₂, dispergiranih v vodi

Sample name	GLYMO/TiO₂ (/)
A	0/1
B	0.1/1
C	1/1
D	2/1

procedure. First, TiO$_2$ nanopowder in dispersion with wetting and defoaming agent was milled for 1,5 hour at 25 °C with organic surface active agent with zirconia balls 1 mm diameter. Than silane coupling agent of different concentrations was added as shown in **Table 1** and the dispersion was milled additionally for 1 hour at the same conditions.

2.3 Preparation of clearcoat with integrated rutile crystalline nanoparticles of TiO₂

We prepared clearcoat in the laboratory as described elsewhere[23]. Water based dispersions of TiO$_2$ nano-particles were than added to clearcoat of 0,6 wt. %, stirred at approximatly 1000 rpm for 20 minutes and prepared for the testing.

2.4 Characterization of the samples

Surface morphology of coated sample was studied by scanning electron microscopy (SEM, ZEISS Gemini Supra 35 VP), with a maximum resolution up to 5 nm. Nanoparticles were dried on brass holders by adhesive carbon band with thin layer of gold. The samples were placed in the vacuum chamber of the instrument and then were examined at various magnifications. Grafting of GLYMO on TiO$_2$ nanoparticles was analysed by FT-IR. The infrared spectra of original and modified TiO$_2$ were conducted using a FT-IR spectrometer (PERKIN ELMER Spectrum 100) and thermogravimetrical analysis by TGA/DSC 1, METTLER TOLEDO.

Zeta potential was obtained to investigate the surface character of original TiO$_2$ and TiO$_2$ modified with GLYMO. The electro-phoretic mobility data, measured also by Zetasizer Nano series HT by of the dispersions were transformed into ζ-potential according to[25] (eq. 1):

$$\zeta = \left[\frac{4\pi\eta\mu}{\varepsilon} \right] \qquad (1)$$

where ε is a dielectric constant of the dispersing medium and η the solvent viscosity. pH was measured by pH meter (Mettler Toledo).

UV–VIS transmittance of modified samples was measured for estimating UV-shielding ability and trans-parency. 0.6 wt. % of surface treated TiO$_2$ nanoparticles was integrated into acrylic clear coating and 200 μm films were prepared. The different free film systems (coating-UV absorber) were analysed by UV-VIS spec-trophotometer Varian Cary 100. The film transmittance was measured in the wavelength range 280 to 720 nm.

At the end, wood blocks measuring 15 × 7 cm^2 (lon-gitudinal × tangential) × 0,5 cm width were cut from air dried boards from the specie pine. Two layers of clear coat of thickness of 200 μm were applied on pine blocks. Coated wood plates were used to assess weathering exposure degradation (QUV accelerated weathering tester, Q – PANEL LAB PRODUCTS). Simulation of exterior use was done by six weeks weathering by an

optimised cycle defined: 4h at (60 ± 3) °C and 4h water shower at (50 ± 3) °C. Only light of the solar type was activated on the QUV with sources type UVA-340 nm[26]. Gloss at 60° was measured by Micro-TRI-gloss (Byk Gardner).

3 RESULTS AND DISCUSSION

3.1 SEM characterization

The size of the nanoparticles, grafted with GLYMO was analysed by scanning electron microsope (SEM). SEM images at two different magnifations of sample C are shown on **Figure 1**. Agglomeration tendency of TiO₂ nanoparticles in the dispersion cannot be determined because of the preparation of the sample, however we assume, that some agglomerates are probably present as seen on SEM image. Individual particles can be identified, which appears to be polydisperse in size but below 100 nm.

3.2 TGA analysis

To estimate the amount of GLYMO grafted on nanoparticles, the various percentage of GLYMO – grafted nano-TiO₂ particles were analyzed by TGA technique. **Figure 2** shows the TGA curves of untreated TiO₂ nanoparticle, GLYMO alone and treated TiO₂ nanoparticles with different percentages of GLYMO. For untreated nanoparticles (sample A), the weight loss from 120 till 600 °C is almost negligible and is probably due to desorption of physisorbed water [27]. For GLYMO alone the weight loss begins at 120 °C and ends at 200 °C. As can be seen for sample B, C and D, the various weight percentages of GLYMO grafted nanoparticles show sharp weight loss, beginning near 220 °C, continues till 620 °C, which is a consequence of oxidative thermal decomposition of grafted GLYMO as quantitatively
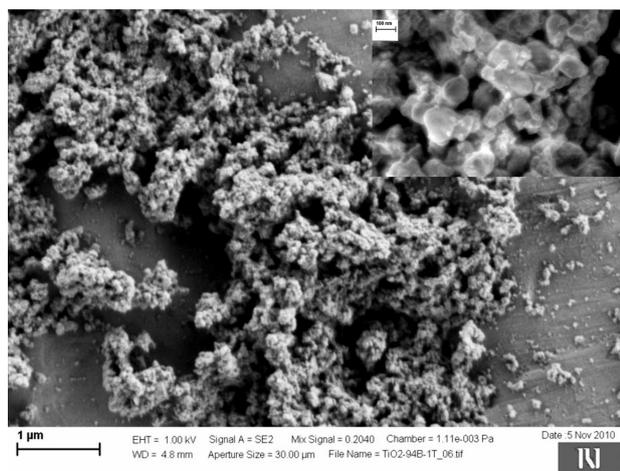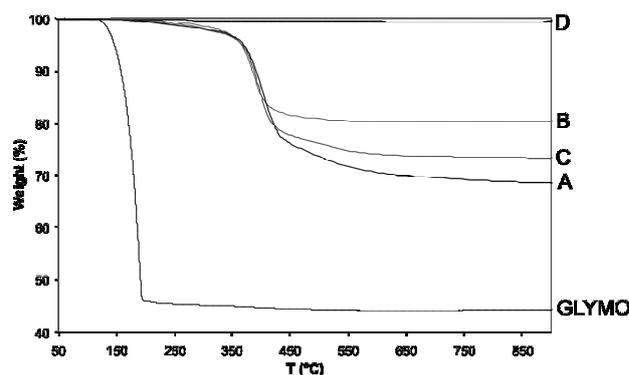

Figure 2: TGA curves of untreated TiO₂ nano-particle (sample A) and treated TiO₂ nano-particle (sample B–D). The composition of all samples is described in **Table 1**.
Slika 2: TGA krivulje površinsko neobdelanih (vzorec A) ter površinsko obdelanih (vzorci B–D) nanodelcev TiO₂. Sestava vseh vzorcev je podana v **Tabeli 1**.

shown in **Table 2**. The largest amount of grafted GLYMO was in the case of sample C.

Table 2: TGA-based weight losses caused by grafting of GLYMO and the amount grafted/added GLYMO of various GLYMO – grafted nanoparticles TiO₂. The composition of all samples is described in **Table 1**.
Tabela 2: Izguba mase vzorcev nanodelcev TiO₂ ter razmerje vezan/dodan GLYMO površinsko obdelanih in neobdelanih z GLYMO glede na TGA analizo. Sestava vseh vzorcev je podana v **Tabeli 1**.

Sample	GLYMO:TiO₂ (/)	Weight loss caused by grafting of GLYMO	The amount grafted/added GLYMO (%)
A	0	/	/
B	0,1	1,00	67
C	1	11,40	76
D	2	20,20	67
GLYMO	/	/	/

3.3 FTIR spectroscopy

The hydroxyl groups on the surface of the TiO₂ nanoparticles (TiOH) are reactive sites for the reaction with alkoxy groups of silane compounds, however corresponding bands are not present in spectrum of unmodified TiO₂, since it was dried at 130 °C for 24h. The efficiency of silane grafting on TiO₂ nano-particles was determined by Fourier transform infrared spectro-scopy (FTIR). **Figure 3** shows normalised FTIR spectra of unmodified TiO₂ nanoparticles (sample A), grafted TiO₂ nanoparticles with GLYMO (sample B – D), GLYMO alone and GLYMO with addition of water. In the spectra of all TiO₂ nano-particles the broad band between 400 and 800 cm⁻¹ correspond to Ti–O–Ti network. GLYMO posseses two functional groups: epoxi and metoxysilyl, which both hydrolize and condensate. Epoxy band in FTIR spectra is preserved, while the intensity of Si-O-Me band is decreased. Also two bands of hydroxyl groups appear at ~3300 and ~1640 cm⁻¹ because of hydrolysis of Si-O-Me groups. In spectra of

Figure 1: SEM image of sample C with inserted image at higher magnification
Slika 1: SEM posnetek vzorca C z vstavljenim posnetkom pri višji povečavi

GLYMO with addition of water peak at 1050 cm^{-1} appears, which we can assign to formation of Si-O-Si groups. Compared with the spectrum of non-modified TiO$_2$, FTIR spectrum of GLYMO modified sample exhibits some new characteristic absorption peaks. Peak at ~1200 and 1093 cm^{-1} which belongs to Si-O-Me groups[28,29], was observed in the spectra of samples C and D, however not in the spectruum of sample B, which indicates that only in the case of sample B complete hydrolysis and condensation of GLYMO takes place. In contrast to GLYMO spectruum, we cannot observe in GLYMO modified TiO$_2$ spectra peak at 914 and 1254 cm^{-1} which corresponds to epoxi group[30–34]. We presume that the epoxi group opens and reacts with -OH groups which were formed by the hydrolysis of metoxysilyl groups. The broad bend at ~1050 cm^{-1} represent the Si-O-Si bond is observed which indicates the formation of Si-matrix[35]. The small peak in spectra of samples B – D at around 930 cm^{-1} reconfirms condensation reaction between methoxysilyl groups of GLYMO and the TiO$_2$ surface hydroxyl groups[36,8].

To sum up, Si-O-Me groups of GLYMO have reacted completley only in the case of sample B, in samples C and D are still present. Epoxi groups of GLYMO have reacted completely in all GLYMO modified TiO$_2$ nanoparticles samples. The results of FTIR analysis confirm that Si-O-Si network has been formed probably around the TiO$_2$ nanoparticles and in small amount Si-atoms of GLYMO are bound to TiO$_2$ surface. Similarly, F. Bauer and coauthors reported about a polymerization-active siloxane shell formed around the nanoparticles Al$_2$O$_3$, when surface treated by GLYMO[37]. The reaction of GLYMO with TiO$_2$ nanoparticles leads to different kind of stabilization of nanoparticles in the dispersion as suggested by the producers of GLYMO, since they claim that in the presence of water the methoxysilyl groups hydrolyze to form reactive silanol groups which bound to inorganic substance[24].

3.4 pH and ζ-potencial measurement

pH and ζ-potential measurement were used to quantify the conditions leading to the stability of TiO$_2$ dispersions. Relevant values of the pH – measurements and ζ-potential of unmodified and modified TiO$_2$ with GLYMO are collected in **Table 3** and in **Figure 4**. The pH variation from 4,6 to 5,9 upon adsorption of GLYMO was detected. An increase of the pH from 5,6 up to 5,94 when increasing GLYMO/TiO$_2$ from 0 to 1 (sample A, B and C) was accompanied with an increase of ζ-potential from ~-33 to around ~-39 mV, with subsequent increase in colloid stability. We assume that TiO$_2$ surface is probably mostly covered with modifier in monolayer. As ratio GLYMO/TiO$_2$ increases to 2, the pH decreases to 5,43, resulting in decrease in zeta potential to -35,5 mV. We predict that the reason for decrease in pH and ζ-potential is the excess amount of GLYMO or formatation of multilayer on TiO$_2$ surface as observed by E. Ukaji et. al.[8]. It is supposed that thicker layer could be formed due to subsequent growth of layer to dimers, oligomers, and polymers.

Table 3: pH values for TiO$_2$ dispersions, in the presence of different amounts of GLYMO (sample A–D). The composition of all samples is described in **Table 1**.
Tabela 3: pH vrednosti disperzij TiO$_2$ v prisotnosti različnih deležev GLYMO (vzorec A–D). Sestava vseh vzorcev je podana v **Tabeli 1**.

Sample name	pH
A	5,60
B	5,78
C	5,94
D	5,43

3.5 Ageing behaviour

Artificial weathering results in surface degradation of the coatings, which affect the appearance of the coating,
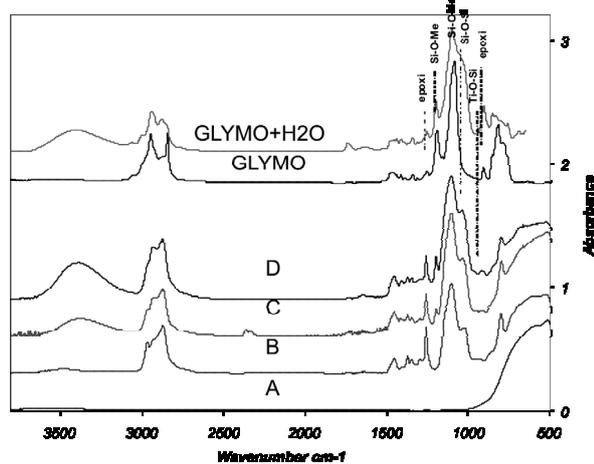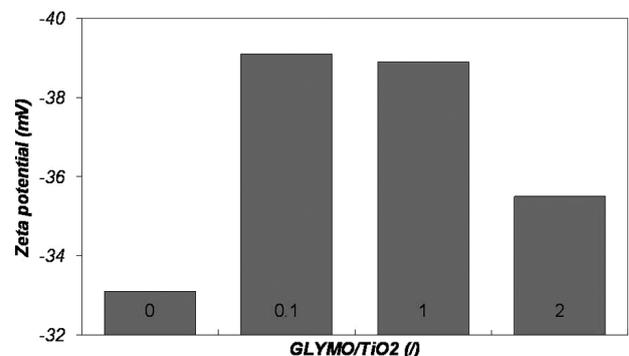

Figure 3: FTIR spectra of untreated nano-TiO$_2$ (sample A), grafted TiO$_2$ nano-particles with GLYMO (sample B–D), pure GLYMO and GLYMO with addition of water. The composition of all samples is described in **Table 1**.
Slika 3: FTIR spektri neobdelanega nano-TiO$_2$ (vzorec A), površinsko obdelanih nanodelcev TiO$_2$ z GLYMO (vzorec B–D), samo GLYMO, GLYMO z dodatkom vode. Sestava vseh vzorcev je podana v **Tabeli 1**.

Figure 4: Zeta potential measurement vs. ratio GLYMO/TiO$_2$
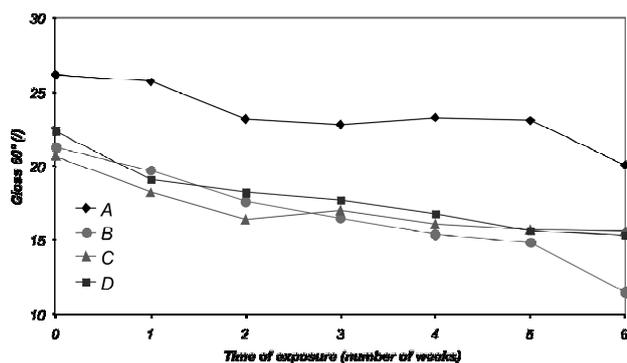**Slika 4:** Diagram meritev zeta potenciala v odvisnosti od razmerja GLYMO/TiO$_2$

Figure 5: Gloss measurement vs. irradiation time in a QUV apparatus for the exterior use clearcotings with different UV absorbers, samples A–D, with their composition described in **Table 1**
Slika 5: Meritve sijaja v odvisnosti od časa izpostave v UV komori za premaz za zunanjo uporabo z različnimi UV absorberji, vzorci A–D, njhova sestava je podana v **Tabeli 1**

is the information on photostabilisation performances of UV absorbers[8,38,39]. M. Beyer and C. Jobos investigated the use of nano-scale light absorbers in water based glaze for outdoor applications. They showed that TiO$_2$ proved to be effective additives[6] in concentration 0,25 – 4 wt. % TiO$_2$ [9].

For outdoor weathering simulation of clearcoating gloss measurement during the exposure in QUV chambre for six weeks are displayed in **Figure 5**. **Figure 5** shows gloss 60° vs. time of exposure in QUV chambre for clearcoating with modified TiO$_2$ nanoparticles of different wt. ratios of GLYMO/TiO$_2$. The results illustrated that addition of GLYMO decreases the gloss 60°. During accelerated weathering the gloss changes are strongly correlated with the degradation level of the surface coating. In some composite materials the polymer around the filler particles will degrade due to the particle catalytic effect[40]. The accelerated weathering with water spray induced the washing out of degradation products on the coatings surface and consequently a fresh surface was further exposed. During the accelerated weathering a pronounced loss of gloss was observed for coatings formulated with nanoparticle UV absorber[41]. We can conclude that the surface treatemtnof TiO$_2$ nanoparticles with GLYMO reduces the gloss 60° of acrylic coating before exposure to accelerated weathering. The gloss change after six week exposure to accelerated weathering is the smalest in the case of sample C, which shows that the UV efficiency was improved the most, when ratio GLYMO/TiO$_2$ was 1.

4 CONCLUSIONS

Surface modification and characterization of TiO$_2$ nano-particles with GLYMO at different wt. percentages as an additive in a polyacrylic clear coating were investigated. TGA and FTIR analysis show that grafting of GLYMO on the nano-particles has occurred successfully. According to ζ-potential measurements the most

stable TiO$_2$ nanoparticle dispersions are with ratio GLYMO:TiO$_2$ 0,1 and 1. At the end, artificial weathering results confirm that surface treatment of TiO$_2$ nanoparticles with GLYMO with ratio GLYMO:TiO$_2$ = 1 improves nanoparticles dispersion and consequently its transparency the most and improves UV protection of acrylic clear coating.

Acknowledgement

5 REFERENCES

[1] A. L. Linsebigler, G. Lu, J. T. Yates, Photocatalysis on TiO$_2$ surfaces: principles, mechanisms, and selected results, Chem. Rev. 95 (**1995**), 735–758

[2] H. Choi, Y.J. Kim, R.S. Varma, D.D. Dionysiou, Thermally stable nanocrystalline TiO2 photocatalysts synthesized via sol–gel methods modified with ionic liquid and surfactant molecules, Chem. Mater. 18 (**2006**), 5377–5384

[3] U Bach, D. Lupo, P. Comte, J. E. Moser, F. Weissortel, J. Salbeck, H. Spreitzer, M. Gratzel, Solid-state dye-sensitized mesoporous TiO$_2$ solar cells with high photon-to-electron conversion efficiencies, Nature 395 (**1998**), 583–585

[4] M. Anpo, M. Takeuchi, The design and development of highly reactive titanium oxide photocatalysts operating under visible light irradiation, J. Catal. 216 (**2003**), 505–516

[5] H. Y. Yang, S. K. Zhu, N. Pan, Studying the mechanisms of titanium dioxide as ultraviolet blocking additive for films and fabrics by an improved scheme, J. Appl. Polym. Sci. 92 (**2004**), 3201–3210

[6] F. Aloui, A. Ahajji, Y. Irmouli, B. George, B. Charrier, A. Merlin, Inorganic UV absorbers for the photostabilisation of wood-clear-coating systems: comparison with organic UV absorbers, Appl. Surf. Sci. 253 (**2007**), 3737–3745

[7] B. Mahltig, H. Bottcher, K. Rauch, U. Dieckmann, R. Nitsche, T. Fritz, Optimized UV protecting coatings by combination of organic and inorganic UV absorbers, Thin Solid Films 485 (**2005**), 108–114

[8] E. Ukaji, T. Furusawa, M. Sato, N. Suzuki, The effect of surface modification with silane coupling agent on suppressing the photo-catalytic activity of fine TiO$_2$ particles as inorganic UV filter, Appl. Surf. Sci. 254 (**2007**), 563–569

[9] N. S. Allen, M. Edgea, A. Ortega, G. Sandovla, C. M. Liauwa, J. Verrana, Degradation and stabilisation of polymers and coatings: nano versus pigmentary titania particles, Polym. Degrad. Stab. 85 (**2004**), 927–946

[10] M. Sangermano, E. Borlatto, F. D. D' Herin Bytner, A. Priola, G. Rizza, Photostabilization of cationic UV-cured coatings in the presence of nano TiO$_2$, Prog. Org. Coat. 59 (**2007**), 122–125

[11] C. Lu, Z. Cui, J. Guan, B. Yang, J. Shen, Research on Preparation, Structure and Properties of TiO$_2$/Polythiourethane Hybrid Optical Films with High Refractive Index Macromol. Mater. Eng. 288 (**2003**), 717–723

[12] C. Lu, Z. Cui, B. Yang., J. Shen, High refractive index thin films of ZnS/polythiourethane nanocomposites, J. Mater. Chem. 13 (**2003**), 526–530

[13] J. Jordan, K. I. Jacob, R. Tannenbaum, M.A. Sharaf, I. Jasiuk, Experimental trends in polymer nanocomposites—a review, Mater. Sci. Eng. A 393 (1e2) (**2005**), 1

¹⁴ S. Farrokhpay, A review of polymeric dispersant stabilisation of titania pigment, Advances in Colloid and Interface Science, 151 (**2009**), 24–32

¹⁵ O. K. Park, Y. S. Kang, B. G. Jo, Synthesis of TiO₂ nanoparticles coated with SiO2 for suppression of photocatalytic activity and increased dispersion stability, J. Ind. Eng. Chem. 10 (**2004**), 733–738

¹⁶ A. M. El-Toni, S. Yin, T. Sato, Control of silica shell thickness and microporosity of titania–silica core–shell type nanoparticles to depress the photocatalytic activity of titania, J. Colloid Interface Sci. 300 (**2006**), 123–130

¹⁷ O. K. Park, Y. S. Kang, Preparation and characterization of silica-coated TiO₂ nanoparticle, Colloids Surf. A 257–258 (**2005**), 261–265

¹⁸ P. Katangur, P. K. Patra, S. B. Warner, Nanostructured ultraviolet resistant polymer coatings, Polym. Degrad. Stab. 91 (**2006**), 2437–2442

¹⁹ A. M. Djerdjev, J. K. Beattie, R. W. O'Brien, Coating of silica on titania pigment particles examined by electroacoustics and dielectric response, Chem. Mater. 17 (**2005**), 3844–3849

²⁰ J. N. Ryan, M. Elimelech, J. L. Baeseman, R. D. Magelky, Silica-coated titania and zirconia colloids for subsurface transport field experiments, Environ. Sci. Technol 34 (**2000**), 2000–2005

²¹ K. V. P. M. Shafi, A. Ulman, X. Yan, N. L. Yang, M. Himmelhaus, M. Grunze, Sonochemical preparation of silane-coated titania particles, Langmuir 17 (**2001**), 1726–1730

²² M. Sabzi, S.M. Mirabedini, J. Zohuriaan-Mehr, M. Atai, Surface modification of TiO₂ nano-particles with silane coupling agent and investigation of its effect on the properties of polyurethane composite coating, Progress in Organic Coatings 65 (**2009**), 222–228

²³ J. Godnjavec, B. Znoj, P. Venturini, A. Žnidaršič. The application of rutile nano-crystalline titanium dioxide as UV absorber. Inf. MIDEM, 40 (**2010**) 1, 6–9

²⁴ http://svn.assembla.com/svn/camsi-x/src/fe/LITERATURA/Degussa-GLYMO.pdf

²⁵ Adamson AW Physical Chemistry of Surfaces, 5th edn. Wiley, New York, 1991, 218

²⁶ SIST EN ISO 11507:2002

²⁷ L. Jun, J.A. Siddiqui, R. M. Ottenbrite, Surface modification of inorganic oxide particles with silane coupling agent and organic dyes, Polym. Adv. Technol. 12 (**2001**), 285–292

²⁸ I. C. McNeill, M. H. Mohammed, Thermal analysis of blends of low density polyethylene, poly(ethyl acrylate) and ethylene ethyl acrylate copolymer with polydimethylsiloxane, Polymer Degradation and Stability, 50 (**1995**) 3, 285–295

²⁹ Wenxui Que, Y. Zhou, Y. L. Lam, Y. C. Chan, C. H. Kam, Optiocal and microstructural properties of sol-gel derived titania/organically modified silane thin films, Thin Solid Films, 358 (**2000**) 1–2, 16–21

³⁰ J. Macan, H. Ivanković, Influence of hydrolysis conditions on curing and properties of an epoxy-silane based hybrid material, 11. Conference on Materials, Processes, Friction and Wear MATRIB 06, Vela Luka, 22–24. 6. 2006, 99–104

³¹ N. Eidelman, D. Raghavan, A. M. Forster, E. J. Amis, A. Karim, Combinatorial Approach to characterizing epoxy curing, Macromol. Rapid Commun., 25 (**2004**), 259–263

³² http://www.shimadzu.com.br/analitica/aplicacoes/espectrofotometros/ftir/2_22-1.pdf

³³ G. Nikolić, S. Zlatković, M. Cakić, S. Cakić, C. Lacnjevac, Z. Rajic, Fast Fourier transform IR characterization of epoxy GY systems crosslinked with aliphatic and cycloapliphatic EH polyamine adducts, Sensors, 10 (**2010**), 684–696

³⁴ http://www.thefreelibrary.com/Insitu+monitoring+of+the+curing+of+epoxy+resins+by+DSC,+FTIR+and...-a0216041185

³⁵ N. Grošelj, M Gaberšček, U. Opara Krašovec, B. Orel, G. Dražič, P. Judeinstein, Electrical and IR spectroscopic studies of peroxopolytungstic acid/organic–inorganic hybrid gels, Solid State Ionics, 125 (**1999**) 1–4, 125–133

³⁶ Q. Cheng, C. Li, V. Pavlinked, P. Saha, H. Wang, Appl. Surf. Sci. 252 (**2006**), 4154–4160

³⁷ F. Bauer, U. Decker, H. Ernst, M. Findeisen, H. Langguth, R. Mehnert, V. Sauerland and R. Hinterwaldner, Functionalized inorganic/organic nanocomposites as new basic raw materials for adhesives and sealants International, Journal of Adhesion and Adhesives, 26 (**2006**) 7, 567–570

³⁸ M. Sakamoto, H. Okuda, J. Jpn. Soc. Colour. Mater. 68 (**1995**) 4, 203–210

³⁹ Y. Q. Li, S. Y. Fu, Y. Yang, Y. W. Mai, Facile synthesis of highly transparent polymer nanocomposites by introduction of core–shell structured nanoparticles, Chem. Mater. 20 (**2008**), 2637–2643

⁴⁰ A. C. Dodd, A. J. McKinley, M. Saunders, T. Tsuzuki, J. Nanopart. Res. 8 (**2006**), 43–51

⁴¹ M. V. Cristeaa, B. Riedla, P. Blancheta, Enhancing the performance of exterior waterborne coatings for wood by inorganic nanosized UV absorbers, Progress in Organic Coatings, 69 (**2010**), 432–441